

Control Of A Dc Motor Using Active Disturbance Rejection

MSc. Fernando Jesús Regino Ubarnes¹, Msc July Andrea Gómez Camperos^{2*}, MSc. Haidee Yulady Jaramillo³

¹ Universidad Francisco de Paula Santander Seccional Ocaña, Facultad de Ingeniería, Grupo de Investigación (GINSTI) Ocaña, Norte de Santander, Colombia.

² Universidad Francisco de Paula Santander Seccional Ocaña, Estudiante de Doctorado en Automática de la Universidad de Pamplona, Facultad de Ingeniería, Grupo de Investigación (GINSTI) Ocaña, Norte de Santander, Colombia.

³ Universidad Francisco de Paula Santander Seccional Ocaña, Estudiante de Doctorado Universidad Francisco Pontificia Bolivariana, Facultad de Ingeniería, Grupo de Investigación (GINSTI) Ocaña, Norte de Santander, Colombia.

E-mail*: July Andrea Gómez Camperos

ABSTRACT:

This paper presents the design of a proportional integral derivative control strategy applied to the speed control of a direct current motor, this was measured the ability of the system to follow a reference signal of step type. The measurement was made in the frame of the mean square error percentage where the degree of the polynomial with which the disturbance is approximated was varied, giving as a result for $m=2$ a mean square error percentage of 2.35%, for $m=4$ a mean square error percentage of 1.23% and finally for $m=6$ a mean square error percentage of 0.87%.

Keywords: Active disturbance rejection, control, modeling, speed control, tracking error

INTRODUCTION

Due to the variety of technical configurations, direct current (DC) motors are an integral part of various applications and are used in different industries (Guerrero et al., 2020). Especially the relatively simple speed and torque control, precise controllability and efficiency enable a wide range of applications (Zhu, 2022). As a conventional and proven motor type, brushed DC motors require few or no external components, which also makes them more useful under harsh environmental conditions (Sahana et al., 2016). Suitable applications include rotating and grinding machines, conveyor systems and vacuum cleaners. In addition, brushed DC motors can be used to drive compressors, rotating machines and elevators (Buzi & Marango, 2013; Lu Renquan et al., 2008; Mozaffari Niapour et al., 2014; Sadiq et al., 2013). For the case study a DC motor with a constant magnetic field is presented as shown in Figure 1.

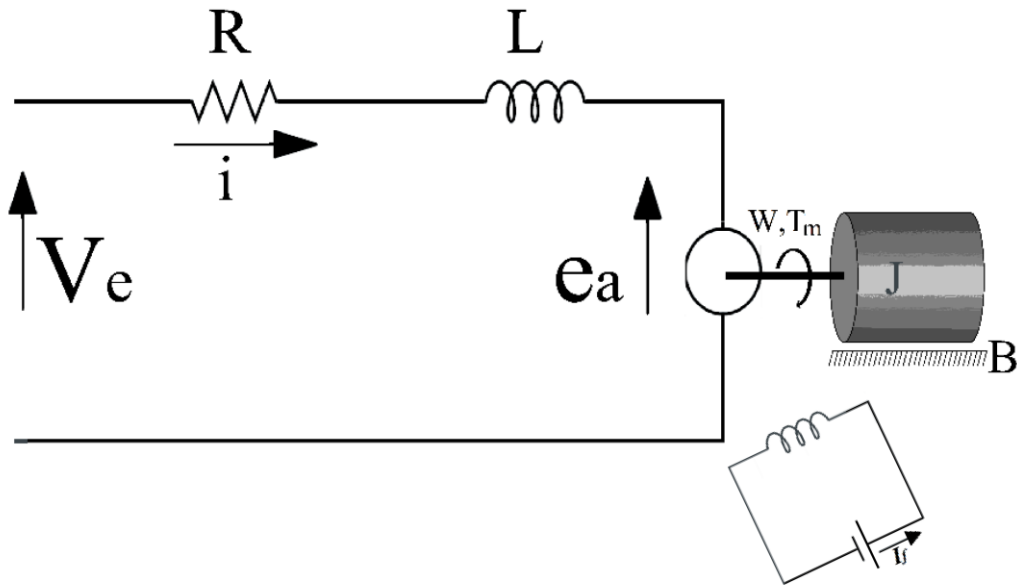


Figure 1. Schematic diagram of direct current motor

MATERIALS AND METHODS

This section presents the mathematical model of the DC motor, figure 1 shows the schematic diagram of a direct current motor where the DC motor armature is modeled as having a constant resistance R in series with a constant inductance L representing the inductance of the armature coil, and a power supply V , representing the voltage generated in the armature, which for this case $R=0.8\Omega, L=750\text{mH}$. Where $E_a(t)$ is the counter electromotive force, by applying Kirchhoff's voltage law the circuit equation is as follows.

$$v(t) = Ri(t) + L \frac{di(t)}{dt} + E_a(t)$$

$$L \frac{di(t)}{dt} = v(t) - Ri(t) - E_a(t) \quad (1)$$

The equation of the mechanical section is given by the model

$$T_m(t) = J \frac{d\omega(t)}{dt} + B\omega(t)$$

$$J \frac{d\omega(t)}{dt} = T_m(t) - B\omega(t) \quad (2)$$

Where $T_m(t)$ is the torque of the DC motor, B is the coefficient of friction equivalent to the DC motor and load mounted on the motor shaft, J is the total moment of inertia of the rotor and load relative to the motor shaft, $\omega(t)$ is the angular velocity of the motor and $\frac{d\omega(t)}{dt}$ is the angular acceleration. For this case $B=0.15\text{N.m.s}$, $J=0.01\text{Kg.m}^2$

The angular velocity has a direct relationship with the counter electromotive force, this is given by equation 3 where K_a is known as the counter electromotive constant which in this case is $K_a = 2.8 \times 10^{-3} \frac{\text{V}}{\text{rad/s}}$.

$$E_a(t) = K_a\omega(t) \quad (3)$$

In the same way the current has a direct relationship with the torque given by equation 4 where K_m is the torque constant which in this case is $K_m = 1.2 \times 10^{-3} \frac{\text{N.m}}{\text{A}}$.

$$T_m(t) = K_m i(t) \quad (4)$$

Moving to the frequency domain, applying the Laplace transform, the transfer function of the angular velocity as a function of the input voltage is given.

$$\frac{\omega(s)}{V(s)} = \frac{K_m}{LJs^2 + (RJ + LB)s + RB + K_m K_a} \quad (5)$$

Thus the transfer function of the proposed DC motor is given by:

$$\frac{\omega(s)}{V(s)} = \frac{0.0012}{0.0075s^2 + 0.1205s + 0.12} \quad (6)$$

GPI CONTROL DESIGN AND SIMULATION RESULTS

According to (Regino et al., 2019) equation (5) has the structure of a perturbed linear system represented by equation 7, where $\kappa = \frac{K_m}{LJ}$ and $\xi(t)$ groups the unmodeled dynamics, endogenous and exogenous perturbations of the system (Lee & Kwok, s/f).

$$y^{(n)}(t) = \kappa u(t) + \xi(t) \quad (7)$$

For the generalized proportional-integral (GPI) control strategy the control action U is given by equation 8 (Regino-Ubarnes et al., 2019).

$$U = \frac{1}{\kappa} \left[y^{*(n)} + \left(\frac{K_{n+m}s^{n+m} + \dots + K_1s + K_0}{s^{m+1}(s^{n-1} + K_{2n+m-1}s^{n-2} + \dots + K_{n+m+1})} \right) (y^* - y) \right] \quad (8)$$

Where n represents the order of the system, which in this case n=2, m is the order of the polynomial with which the disturbance is approximated, y^* is the reference signal and y is the output of the system, which in this case is the angular velocity of the direct current motor. Initially the control strategy will be designed for an order of the polynomial of approximation of the disturbance $m = 2$, then equation 8 is as follows.

$$U = \frac{1}{\kappa} \left[y^{*(2)} + \left(\frac{K_4s^4 + K_3s^3 + K_2s^2 + K_1s + K_0}{s^3(s^1 + K_5)} \right) (y^* - y) \right] \quad (9)$$

Figure 2 represents the system response to a step-type signal, where the poles of the characteristic polynomial are [-7.5 -12.5 -17.5 -22.5 -22.5 -27.5 -30]. To measure the signal tracking, the percent mean square error (PECM) between the reference signal data and the output was applied resulting in a percent error of 2.35%.

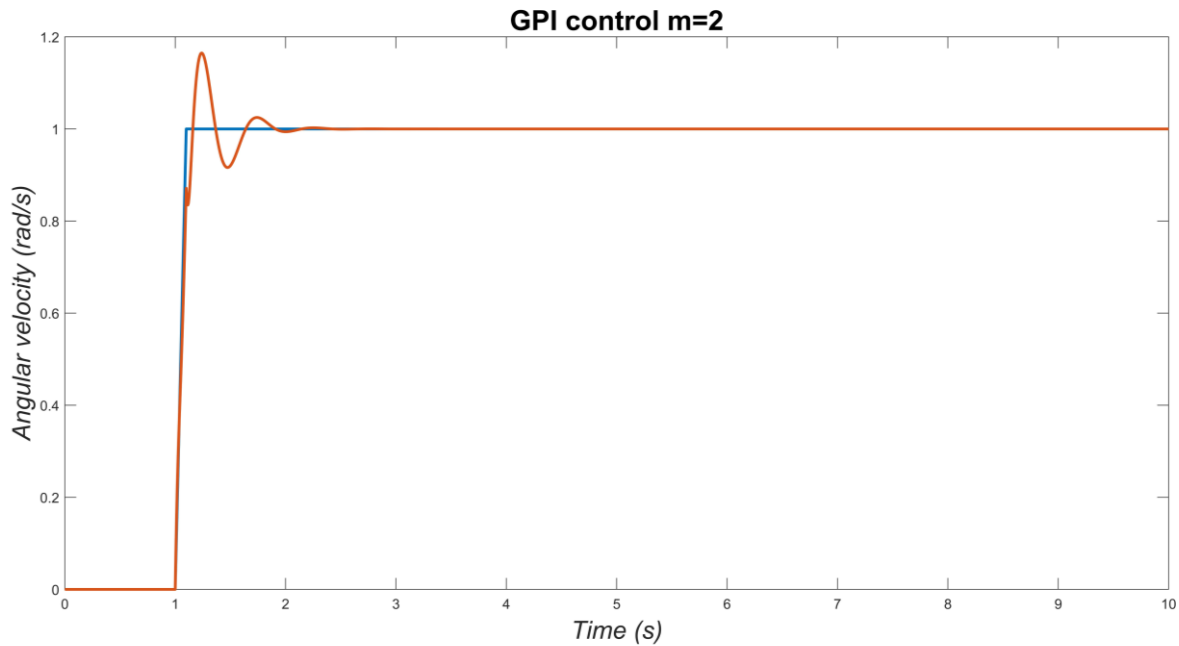


Figure 2. The system response to a step-type signal for m=2

The control strategy for an order of the polynomial of approximation of the perturbation m=4, is as follows.

$$U = \frac{1}{K} \left[y^{*(2)} + \left(\frac{K_6 s^6 + K_5 s^5 + K_4 s^4 + K_3 s^3 + K_2 s^2 + K_1 s + K_0}{s^5 (s^1 + K_7)} \right) (y^* - y) \right] \quad (10)$$

Figure 3 represents the system response to a step type signal, where the poles of the characteristic polynomial are [-15 -25 -35 -45 -55 -55 -60 -65 -70], resulting in an error percentage of 1.23%.

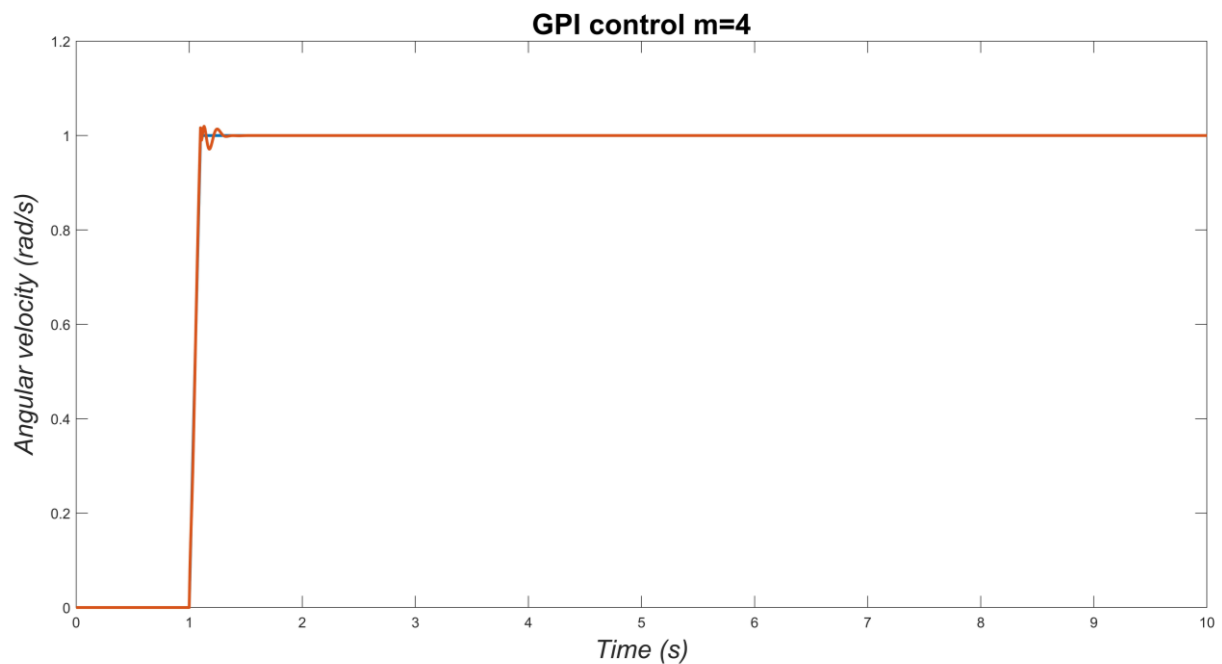


Figure 3. The system response to a step-type signal for m=4

The control strategy for an order of the polynomial of approximation of the perturbation m=6, is

as follows.

$$U = \frac{1}{K} \left[y^{*(2)} + \left(\frac{K_8 s^8 + K_7 s^7 + K_6 s^6 + K_5 s^5 + K_4 s^4 + K_3 s^3 + K_2 s^2 + K_1 s + K_0}{s^7 (s^1 + K_9)} \right) (y^* - y) \right] \quad (11)$$

Figure 4 represents the system response to a step type signal, where the poles of the characteristic polynomial are [-15 -25 -35 -45 -55 -55 -60 -65 -70 -75 -80], resulting in an error percentage of 0.87%

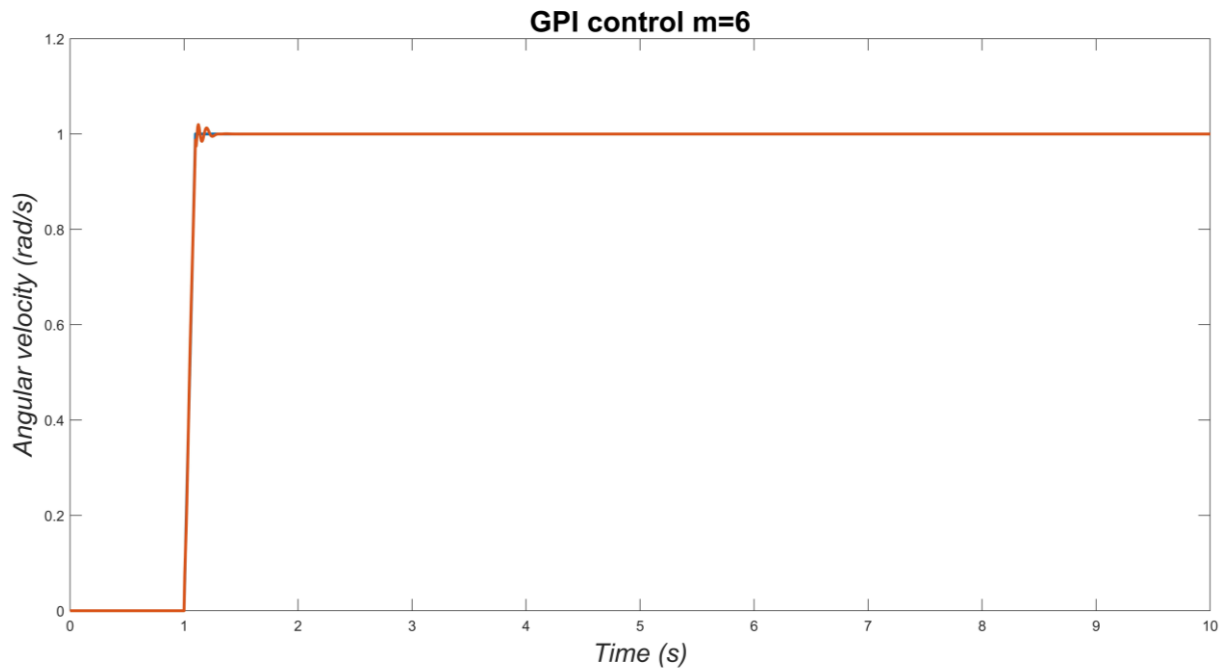


Figure 4. The system response to a step-type signal for m=6

CONCLUSIONS

The control strategies based on the active rejection of disturbances such as GPI control, have substantial advantages over a traditional control strategy such as PID control, this is evidenced in the tracking error, where the GPI control obtained a percentage of mean square error less than unity.

The two control strategies meet the objectives, in terms of parameter variation the GPI control has a superior performance, since with a variation of 50% in the model, the mean square error percentage was less than 3%. This is a good indicator of robustness to the uncertainty that the system model could present.

REFERENCES

- Buzi, E., & Marango, P. (2013). A Comparison of conventional and nonconventional methods of DC motor speed control. *IFAC Proceedings Volumes*, 46(8), 50–53. <https://doi.org/10.3182/20130606-3-XK-4037.00054>
- Guerrero, C., Santibanez, V., Araiza-Olvera, Y., Ibarra-Figueroa, E., & Perez-Perez, B. (2020). Control of velocity of DC motors by classical and passivity methods measuring only position: Theory and experimental comparison. *IEEE Latin America Transactions*, 18(05), 962–970. <https://doi.org/10.1109/TLA.2020.9082926>
- Lee, C. K., & Kwok, N. M. (s/f). Disturbance rejection in a brushless DC motor velocity control system using a variable structure controller. *Proceedings of IEEE International Conference on Control and Applications*, 709–714. <https://doi.org/10.1109/CCA.1993.348320>
- Lu Renquan, Li Shukui, Xue Lin, & Xue Anke. (2008). Robust H_∞ optimal speed control of linear DC motor. *2008 27th Chinese Control Conference*, 743–747. <https://doi.org/10.1109/CHICC.2008.4605448>
- Mozaffari Niapour, S. A. K., Tabarraie, M., & Feyzi, M. R. (2014). A new robust speed-sensorless control strategy for high-performance brushless DC motor drives with reduced torque ripple. *Control Engineering Practice*, 24, 42–54. <https://doi.org/10.1016/j.conengprac.2013.11.014>
- Regino-Ubarnes, F. J., Gómez-Camperos, J. A., & Ruedas-Rodríguez, A. F. (2019). Development of a generalized proportional integral control strategy for level control in a coupled tank system. *Journal of Physics: Conference Series*, 1418(1). <https://doi.org/10.1088/1742-6596/1418/1/012016>
- Regino, F. J., Gomez, J. A., & Espinel, Y. E. E. (2019). Comparative study of three control techniques for the current loop of a Boost Bridgeless converter. *IEEE ICA-ACCA 2018 - IEEE International Conference on Automation/23rd Congress of the Chilean Association of Automatic Control: Towards an Industry 4.0 - Proceedings*, 1–7. <https://doi.org/10.1109/ICA-ACCA.2018.8609810>
- Sadiq, A. A., Bakare, G. A., Anene, E. C., & Mamman, H. B. (2013). A Fuzzy-Based Speed Control of DC Motor Using Combined Armature Voltage and Field Current. *IFAC Proceedings Volumes*, 46(20), 387–392. <https://doi.org/10.3182/20130902-3-CN-3020.00146>
- Sahana, M., Angadi, S., & Raju, A. B. (2016). Speed control of separately excited DC motor using class a chopper. *2016 International Conference on Circuits, Controls, Communications and Computing (I4C)*, 1–6. <https://doi.org/10.1109/CIMCA.2016.8053296>
- Zhu, H. (2022). Research on PLC DC Motor Speed Control System Based on Quantum Fuzzy Control Algorithm. *2022 International Conference on Applied Artificial Intelligence and Computing (ICAAIC)*, 1672–1675. <https://doi.org/10.1109/ICAAIC53929.2022.9793235>